Hindawi
Journal of Chemistry
Volume 2019, Article ID 2924548, 10 pages
https://doi.org/10.1155/2019/2924548

Research Article

Simultaneous Purification and Separation of Syringoside and Oleuropein from *Syringa oblata* Lindl. Extract Using Macroporous Resin

Guoliang Li, Hongxiu Yan, and Xiangping Liu

College of Animal Science and Veterinary Medicine, Heilongjiang Bayi Agricultural University, Daqing 163319, China

Correspondence should be addressed to Xiangping Liu; lxp110@hotmail.com

Received 22 February 2019; Revised 25 July 2019; Accepted 28 August 2019; Published 12 September 2019

Academic Editor: Yun Wei

This study developed an efficient method to simultaneously separate and purify syringoside and oleuropein from *Syringa oblata* Lindl. extract using macroporous resins. The adsorption and desorption property of 11 resins were systematically evaluated. Based on the adsorption performance, HPD-100B resin was selected for the separation of syringoside and oleuropein. The HPD-100B resin fitted well to the Langmuir isotherm model ($R^2 > 0.97$), as ascertained by the results of the static adsorption experiment. Kinetic and dynamic adsorption/desorption experiments were conducted using the HPD-100B resin to optimize the separation parameters of syringoside and oleuropein. On the optimal parameters, syringoside and oleuropein were obtained from the 20% and 40% ethanol eluates, respectively. In addition, the adsorption effluent (15–60 BV) contained a large amount of syringoside with less impurities; therefore, this part was also collected for further syringoside separation and enrichment of syringoside. By only one cycle treatment, the syringoside and oleuropein contents in the final products increased by 7.1-fold and 8.2-fold, respectively, compared to the initial extract. The method developed in this study provides a potential basis for the industrial-scale enrichment and separation of syringoside and oleuropein from *S. oblata* extract.

1. Introduction

Syringoside (also termed syringin or eleutheroside B, Figure 1) is the main active lignan in *Acanthopanax senticosus*. It possesses multiple biological activities, such as hypoglycemic effect [1], antioxidant activity [2], immunomodulatory effect [3], anti-inflammatory and antinociceptive effects [4], hypotensive action [5], sleep-potentiating effects [6], and hepatoprotective effects [7]. Oleuropein (Figure 1) is an important phenolic substance obtained from olive leaves and fruits. The biological and pharmacological activities of oleuropein include antioxidant activity [8], antimicrobial activity [9], anti-inflammatory and analgesic activities [10], cancer prevention and treatment [11, 12], and cardioprotective and neuroprotective effects [13]. Oleuropein can also be used to prevent skin damage and skin cancer caused by UVB radiation [14, 15]; therefore, it has been widely applied in the field of cosmetics. Although the syringoside and oleuropein content are high in *Acanthopanax senticosus* and *Olea europaea* L., respectively, *A. senticosus* only inhabits northern Asia and the Russian Far East, while *O. europaea* can only be cultivated in the Mediterranean region. Consequently, commercial availability of syringoside and oleuropein is limited. In view of the importance of syringoside and oleuropein, finding their alternative sources is very significant.

Syringa oblata Lindl., an ornamental woody plant, is widely distributed in the temperate regions of the world. Its stem is used in traditional Chinese medicine to treat diarrhea and hepatitis. Studies have shown that its stems are rich in syringoside and oleuropein [16].

Many methods have been used for the separation and enrichment of syringoside and oleuropein from *A. senticosus* and *O. europaea*, respectively, including liquid-liquid partition chromatography [17], high-speed counter-current chromatography [18], and silica gel column chromatography [19]. However, these methods have a low separation efficiency, are time-consuming, consume large amounts of organic solvents, and cause environmental pollution; thus,

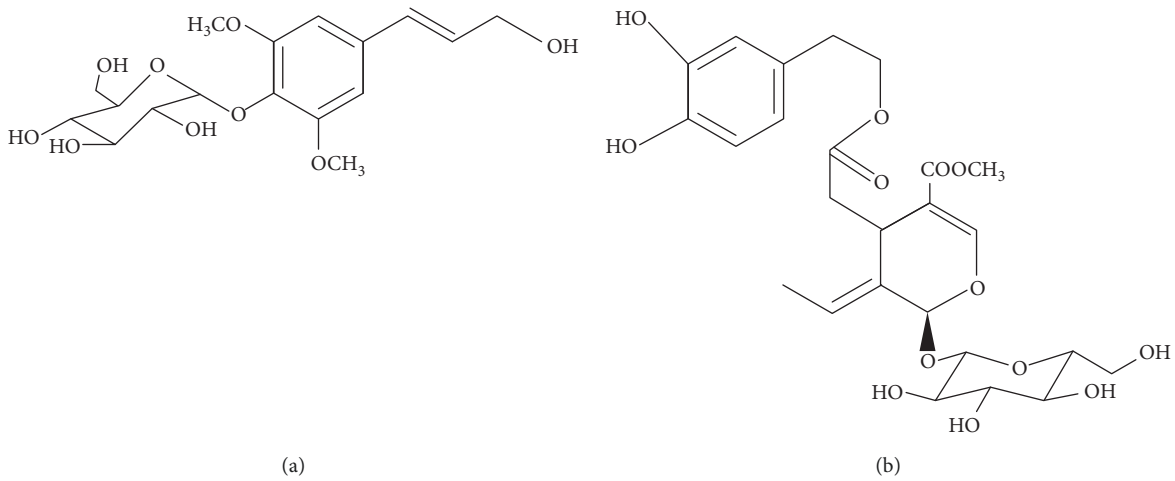

(a) (b)

Figure 1: Chemical structure of (a) syringoside and (b) oleuropein.

their industrial application is limited. Combining the adsorption mechanism and screening principle of resins, different organic compounds can be separated according to their adsorption capacity and molecular weight [20, 21]. Compared with other separation methods, the macroporous adsorption resin method has a larger adsorption capacity, better selectivity, faster adsorption, mild desorption conditions, convenient regeneration, simpler operation, lower cost, and reusability [22, 23]. The separation and enrichment of the active ingredients from the extracts of plants used in traditional Chinese medicine by macroporous adsorption resin has been widely used [24–26]. Although there are several reports about the extraction and purification of syringoside [27, 28] and oleuropein [29, 30] using diverse methods, respectively, no report on the simultaneous separation and enrichment of syringoside and oleuropein from *S. oblata* extract using macroporous resins has been made.

To identify the most suitable resin, the adsorption and desorption property of 11 macroporous resins were investigated. The adsorption and desorption process parameters were optimized in the HPD-100B macroporous resin for efficient separation and enrichment of syringoside and oleuropein. The results of this study will be significant for the selection of adsorption resins and for the large-scale simultaneous separation and enrichment of syringoside and oleuropein from *S. oblata*.

2. Materials and Methods

2.1. Materials and Reagents. Twigs were harvested from *S. oblata* trees in September 2017, in Daqing suburbs, Heilongjiang Province, China. The twigs were dried at room temperature and milled to a size <0.4 mm. The extraction process was as follows: The ethanol extract was obtained by adding 20 times, 40% ethanol by volume, and extracting for 10 min with the homogenate. After the filtration process, the ethanol extract was evaporated in a rotary evaporator (RE52CS-1, Shanghai Yarong Biochemical Instrument, Shanghai, China) to remove the ethanol for reuse. Then, water was added to the remaining liquid to make it up to its original volume; thereafter, it was stored at 4°C until use. The initial concentrations of syringoside and oleuropein in the crude extract were detected by HPLC.

Standard syringoside and oleuropein were purchased from Sigma-Aldrich (Shanghai, China). Methanol of HPLC grade was purchased from J&K Chemical Ltd. (Beijing, China). Deionized water was used throughout. Ethanol of analytical grade was purchased from Beijing Chemical Reagents Co. (Beijing, China). All the HPLC solvents were filtered through a 0.45 μm nylon membrane prior to use.

Macroporous resins of HPD-100A, HPD-100B, HPD-700, HPD-450, HPD-450A, HPD-400A, HPD-750, DM130, HPD-600, ADS-17, and HPD-417 were purchased from Cangzhou Bon Adsorber Technology Co., Ltd. (Cangzhou, China). The specifications of these macroporous resins are summarized in Table 1. The resins were pretreated by the procedure described by Yang et al. [31].

2.2. HPLC Analysis of Syringoside and Oleuropein. A Waters Millennium 32 system equipped with a Waters 717 automatic sampler and a Waters 2487 UV detector was employed to determine the syringoside and oleuropein contents. Chromatographic separation was conducted on an Agilent Zorbax XDB-C18 column (4.6 × 250 mm^2, 5 μm). The mobile phase was methanol-water-phosphoric acid (33 : 66.8 : 0.2, v/v/v). The wavelength of the UV detector was set as 232 nm. The flow rate was 1 mL/min; the injection volume was 10 μL; and the column temperature was 25°C. Calibration curves for syringoside and oleuropein were established within the concentration range of 0.1–0.5 mg/mL using a standard solution. The regression lines for syringoside and oleuropein were $Y_{\text{syringoside}} = 18914X + 17067$ ($r^2 = 0.9998$, $n = 8$) and $Y_{\text{oleuropein}} = 15677X - 72912$ ($r^2 = 0.9993$, $n = 8$), respectively.

2.3. Static Adsorption and Desorption Experiments

2.3.1. Adsorption Resin Screening. Static adsorption experiments of syringoside and oleuropein on all kinds of

Table 1: Physical properties of the tested resins.

Resin	Surface area (m^2/g)	Average pore diameter (Å)	Particle size (mm)	Polarity	Moisture content (%)
HPD-100A	650–700	95–100	0.30–1.20	Nonpolar	66.67
HPD-100B	500–580	120–160	0.30–1.25	Nonpolar	61.49
HPD-700	650–700	85–90	0.30–1.20	Nonpolar	66.10
HPD-450	500–550	90–110	0.30–1.20	Weak-polar	72.00
HPD-450A	500–550	90–100	0.30–1.25	Middle-polar	72.37
HPD-400A	500–550	85–90	0.30–1.20	Middle-polar	64.06
HPD-750	650–700	85–90	0.30–1.20	Middle-polar	57.58
DM130	500–550	90–100	0.30–1.25	Middle-polar	66.48
HPD-600	550–600	80	0.30–1.20	Polar	69.32
ADS-17	90–150	250–300	0.30–1.25	Hydrogen-bonding	51.06
HPD-417	90–150	250–300	0.30–1.25	Hydrogen-bonding	54.55

macroporous resins were performed as follows: 0.5 g of each pretreated macroporous resin was mixed with 60 mL of the crude extract in a 150 mL flask and then shaken continuously (100 rpm/min) at 25°C for 8 h. The concentrations of syringoside and oleuropein after adsorption were determined by HPLC. After the adsorption equilibrium point, the static desorption experiments were performed as follows: the resins were washed with deionized water, and then, 60 mL of a 90% (v/v) ethanol solution was added to each flask containing the adsorbed resins. The flasks were shaken (100 rpm/min) at 25°C for 8 h to desorb syringoside and oleuropein. The concentrations of syringoside and oleuropein in the desorption solutions were also determined by HPLC. Preliminary screening of the resins was carried out by analyzing and comparing their adsorption capacity, adsorption ratio, and desorption ratio:

$$\text{adsorption capacity } Q_e = \frac{(C_0 - C_e)V_i}{W}, \quad (1)$$

$$\text{adsorption ratio } E = \frac{C_0 - C_e}{C_e} \times 100\%, \quad (2)$$

$$\text{desorption ratio } D = \frac{C_d V_d}{(C_0 - C_e)V_i} \times 100\%, \quad (3)$$

where Q_e is the adsorption capacity (mg/g resin, equation (1)); C_0 and C_e are the initial and equilibrium concentrations of solutes in the solutions, respectively (mg/mL); V_i and V_d are the volumes of the initial sample solution (mL) and desorption solution, respectively (mL); W is the weight of the dry resin (g); E is the adsorption ratio (equation (2)); and D is the desorption ratio (equation (3)). Each type of resin was analyzed three times. Based on the adsorption capacity, adsorption ratio, and desorption ratio, two kinds of resin were selected for further experiments.

2.3.2. Adsorption and Desorption Kinetics. First, 5 g of the selected HPD-100B resin was placed in a separate flask with 540 mL of the crude extract solution. The flask was shaken in an oscillating incubator at 25°C and 100 rpm/min. During the adsorption process, 1 mL of syringoside and oleuropein was sampled at 20, 40, 60, 90, 120, 150, 180, 210, 240, 270, 300, and 360 min. After the adsorption, the two resins were separated into five parts, and 0%, 10%, 20%, 30%, and 40% ethanol (v/v) was added, respectively; thereafter, oscillation at 25°C was performed. The concentrations of syringoside and oleuropein were determined at 0, 5, 10, 15, 20, 30, 40, 50, and 60 min, for the respective portions. According to the adsorption and desorption data of the resins, the adsorption and desorption kinetics curves were drawn.

2.3.3. Adsorption Isotherms. Subsequently, 18 copies of 0.5 g of the optimum HPD-100B resins were divided into three groups. The three groups, each with six crude extracts of different concentrations, were placed in shakers at 25, 35, and 45°C, respectively. After shaking (100 rpm/min) for 6 h, the concentration of syringoside and oleuropein in the supernatant was determined. The adsorption behaviors of syringoside and oleuropein on the HPD-100B resin were described by employing the Freundlich and Langmuir models [32].

Langmuir equation is

$$\frac{C_e}{Q_e} = \frac{C_e}{Q_m} + \frac{1}{K_L Q_m}. \quad (4)$$

Freundlich equation is

$$Q_e = K_F C_e^{1/n}, \quad (5)$$

which can be written in the linearized form as follows:

$$\ln Q_e = \ln K_F + \frac{1}{n} \ln C_e, \quad (6)$$

where Q_e is the adsorption capacity (mg/g); C_e is the equilibrium concentration (mg/mL); Q_m is the theoretically calculated maximum adsorption capacity (mg/g resin); K_L is the Langmuir constant; and K_F and n are the Freundlich constants.

2.4. Dynamic Adsorption and Desorption Experiments. Here, 4 g of the HPD-100B macroporous resin was wetly packed into a 1.2 cm × 40 cm glass column to conduct the dynamic adsorption and desorption experiments. The resin thickness and bed volume (BV) were 16.5 cm and 8 mL, respectively. The sample solutions were supplied through three resin columns at 3 BV/h, 4 BV/h, and 5 BV/h, respectively. The effluent from the column was collected and the concentrations of syringoside and oleuropein were

monitored. The breakthrough points of the two target components were detected according to their concentrations in their respective effluents.

Dynamic desorption experiments were conducted at 3 BV/h, 4 BV/h, and 5 BV/h after the adsorption reached equilibrium. The columns were washed with 2 BV deionized water, and then, eluted with 20% and 40% ethanol solution, successively. The eluents were collected, and the concentrations of syringoside and oleuropein in each part of the desorption solutions were detected by HPLC.

3. Results and Discussion

3.1. Screening of the Macroporous Resin. The adsorption process in the macroporous resins is reversible owing to the difference in the polarity, pore size, and specific surface area of the resins; the adsorption and desorption of the effective components vary. In practical applications, the resin is required to adsorb large amounts of the target components, and the desorption rate is required to be high to ensure the maximum recovery of the effective components. Therefore, 11 macroporous resins were preliminarily screened by static adsorption and desorption experiments.

As shown in Figures 2(a) and 2(b), the capacity of the 11 macroporous resins to adsorb-desorb syringoside and oleuropein is distinct, especially for syringoside. The HPD-100B resins have the highest adsorption capacity and adsorption ratio although their desorption ratio is similar to other resins. HPD-100B is a nonpolar resin (Table 1), and the two targeted components are low polarity compounds. This is consistent with the results of Bilal et al. [33], who reported that nonpolar compounds could easily be adsorbed by nonpolar resins. Compared with syringoside, oleuropein has less polarity. Therefore, HPD-100B has a better adsorption effect on oleuropein. Meanwhile, because the two target components have a high molecular weight, a resin with a larger average pore would be more conducive for adsorption. The average pore of HPD-100B is relatively large; consequently, its adsorption capacity is the highest of all the resins. However, ADS-17 and HPD-417, which have a larger average pore than that of HPD-100B, showed the lowest adsorption capacity. This indicates that the hydrogen-bonding adsorption resins were not suitable for the separation of the compounds. In conclusion, HPD-100B has a higher adsorption capacity for syringoside and oleuropein than the other resins because of its polarity and larger average pore. Therefore, HPD-100B resins were selected to further investigate the adsorption kinetics and separation property of syringoside and oleuropein.

3.2. Adsorption and Desorption Kinetics on HPD-100B. The adsorption of syringoside on the HPD-100B resin reached saturation in about 60 min (Figure 3); however, desorption occurred after the adsorption saturation point, i.e., the adsorption capacity reached the highest point and then decreased slightly. Oleuropein saturated the HPD-100B resin in about 240 min, which was significantly slower than the time it took syringoside to reach saturation. The desorption of syringoside, after the adsorption saturation point, may be due to the competitive adsorption of oleuropein in the same solution system.

As shown in Figures 4(a) and 4(b), syringoside desorbed better than oleuropein at the same ethanol concentration. Syringoside has a good desorption effect on the HPD-100B resin at a low ethanol concentration. Syringoside can be completely desorbed from the HPD-100B resins by 20% ethanol (v/v), while the desorption rate of oleuropein by 20% ethanol is only 23.1% after 60 min; complete desorption of oleuropein requires a higher (>20%) ethanol concentration. The complete desorption of oleuropein on the HPD-100B resin (Figures 3–4(b)) requires more than 40% ethanol. Syringoside and oleuropein can be separated from the HPD-100B by gradient elution with a 20% and 40% ethanol-water solution, respectively. Therefore, the HPD-100B resin is suitable in terms of the adsorption capacity and separation efficiency of the two target components.

3.3. Adsorption Isotherms. The adsorption isotherms of syringoside and oleuropein on HPD-100B at 25, 35, and 45°C are shown in Figure 5. The initial concentrations of syringoside were 0.058, 0.114, 0.221, 0.414, and 0.777 mg/mL; the initial concentrations of oleuropein were 0.051, 0.096, 0.185, 0.372, and 0.791 mg/mL. The adsorption isotherm slope of syringoside was lower than that of oleuropein (Figures 5(a) and 5(d)), which indicated that the HPD-100B resin had a higher adsorption capacity for oleuropein than for syringoside. The slope of the adsorption curve of the two components decreases with increasing solute concentration. Such isotherms indicate that the solvent effect on the adsorption of the solute is negligible, i.e., the solvent does not have strong competitive adsorption. Concurrently, the affinity between the molecule and the resin decreases with increasing solute concentration. The equilibrium capacity of the resin to adsorb the target component decreases with increasing temperature. At the same equilibrium mass concentration, the adsorption capacities decrease with increasing temperature, indicating that the resin adsorption process is exothermic. Low temperatures were more conducive for the absorption.

To describe the experimental data of the adsorption isotherms effectively, the adsorption data of syringoside and oleuropein at different temperatures were fitted to Freundlich and Langmuir adsorption isotherm equations (Table 2). The Freundlich and Langmuir equations are suitable for monolayer adsorption on a uniform surface and adsorption on heterogeneous surfaces, respectively. In the Freundlich equation, $1/n$ values ranging from 0 to 1 shows beneficial adsorption [34]. The $1/n$ values were less than 1, which indicated that the adsorption of syringoside and oleuropein on HPD-100B could take place easily. However, the correlation coefficients (R^2) calculated for the Freundlich model (Figures 5(c) and 5(f)) were lower than those of the Langmuir model (Figures 5(b) and 5(e), over 0.97). According to the correlation coefficients (R^2), the Langmuir models were more suitable for describing the adsorption

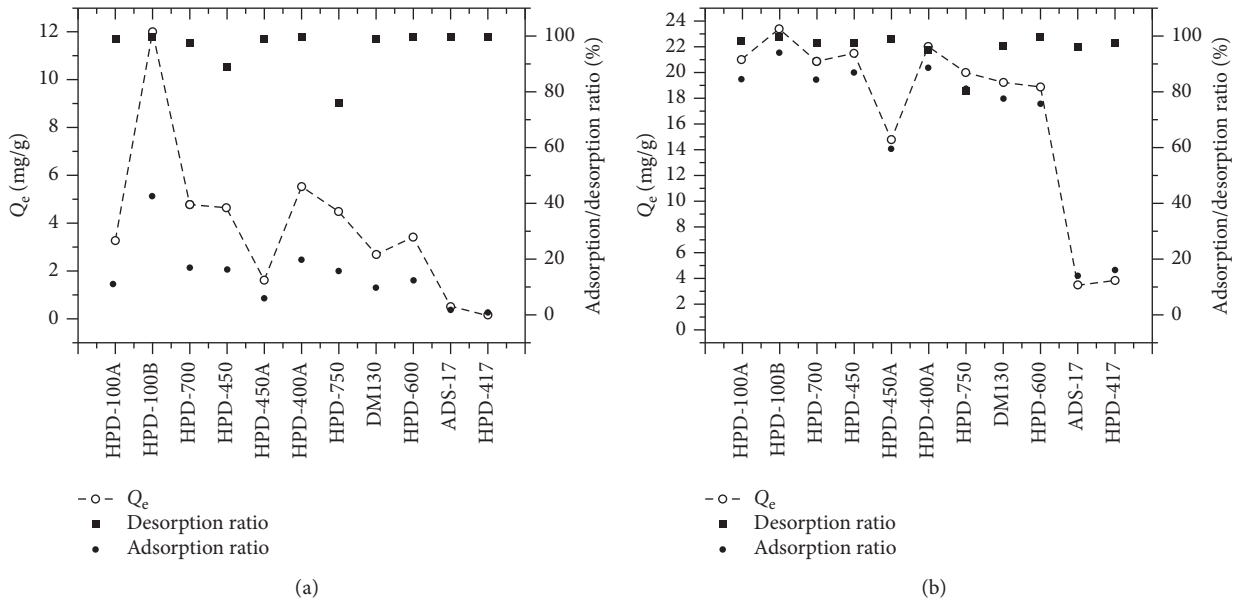

Figure 2: Adsorption capacity (Q_e) and adsorption and desorption ratio of (a) syringoside and (b) oleuropein on different resins.

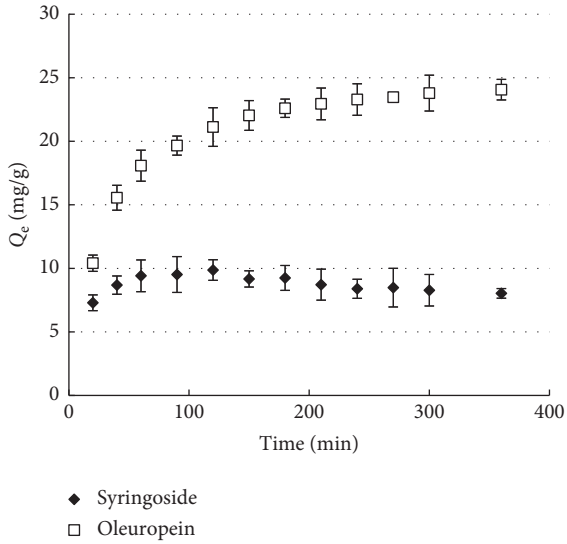

Figure 3: Adsorption kinetics curves of syringoside and oleuropein on the HPD-100B resin.

characteristics of syringoside and oleuropein than the Freundlich models.

The correlation coefficients of the two components at all three temperatures are above 0.97. Considering energy-saving requirement, 25°C was chosen as the final adsorption temperature.

3.4. Dynamic Adsorption and Desorption on the HPD-100B Resin Column. Dynamic experiments were conducted to evaluate the effects of the elution speed on the adsorption and desorption ratio of the resin. When the adsorption saturation of the target component was reached, the adsorption stopped gradually. Corresponding breakthrough curves are necessary to evaluate the relationship between the resin dosage, loading volume of crude extract dosage, and sampling flow rate. The breakthrough curves of syringoside and oleuropein on the HPD-100B resin at different flow rates are shown in Figure 6. When the effluent concentration reaches 10% of the initial sample concentration, adsorption reaches saturation, i.e., the breakthrough point. As shown in Figure 6, the capacities of the HPD-100B resin to adsorb syringoside and oleuropein on its column are quite different. At a 3 BV/h flow rate, syringoside reached the breakthrough point when 14 BV had flowed through the column, and oleuropein reached the breakthrough point when 61 BV had flowed through the column. At the lowest flow rate (3 BV/h), for both components, it took a longer time for the breakthrough point to appear. This may be due to better diffusion of the solute in the sample solution, which is consistent with the report of Charpe and Rathod [35]. Therefore, 3 BV/h was selected as the optimum flow rate.

Considering the breakthrough points of syringoside and oleuropein, the maximum sample loading at 3 BV/h was determined as 122 mL/g of resin. At the breakthrough point, the absorption capacities were 12.2 and 51.5 mg/g for syringoside and oleuropein, respectively.

The dynamic desorption curves of syringoside and oleuropein were obtained by plotting the volume of the eluent against the concentration of the target component in the eluent that was successively eluted by 20% and 40% v/v ethanol-water solution (Figure 7). The syringoside, which was adsorbed on HPD-100B, was almost completely eluted by 20% ethanol, and no syringoside was detected in the subsequent 40% ethanol elution process. In contrast, only a small amount of oleuropein was eluted in 20% ethanol. In general, syringoside and oleuropein in the *S. oblata* extract were successively eluted from the HPD-100B resin by 20% and 40% ethanol, respectively.

It can also be deduced from Figure 7 that elution was best at a low flow rate (3 BV/h); however, too low a flow rate will

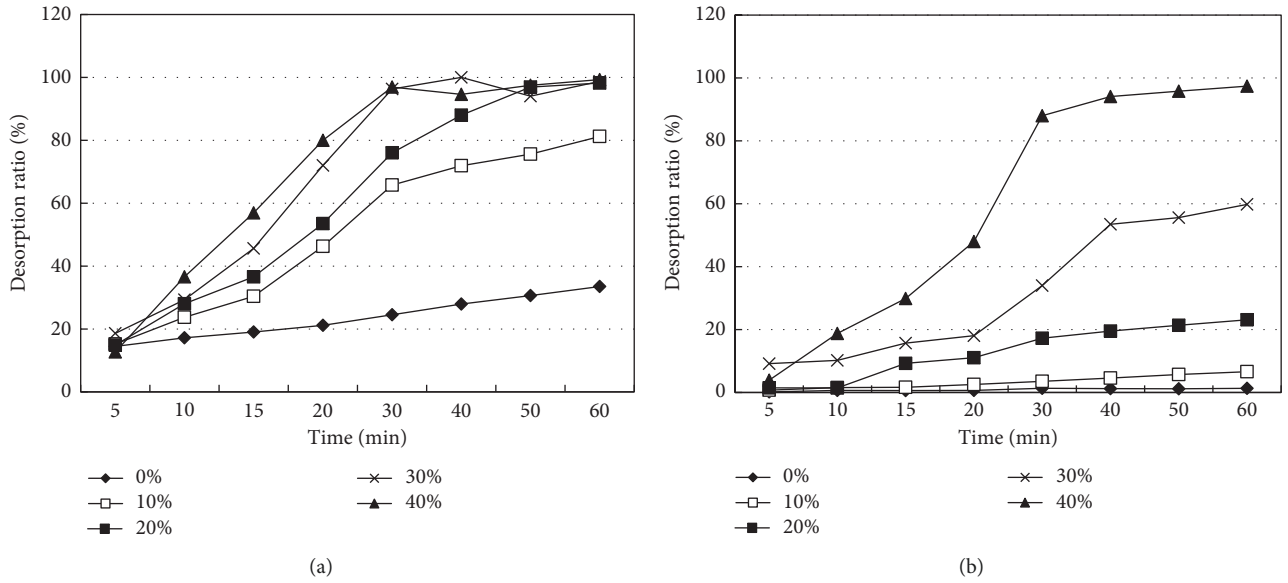

Figure 4: Desorption curves of (a) syringoside and (b) oleuropein in different ethanol concentrations on the HPD-100B resin.

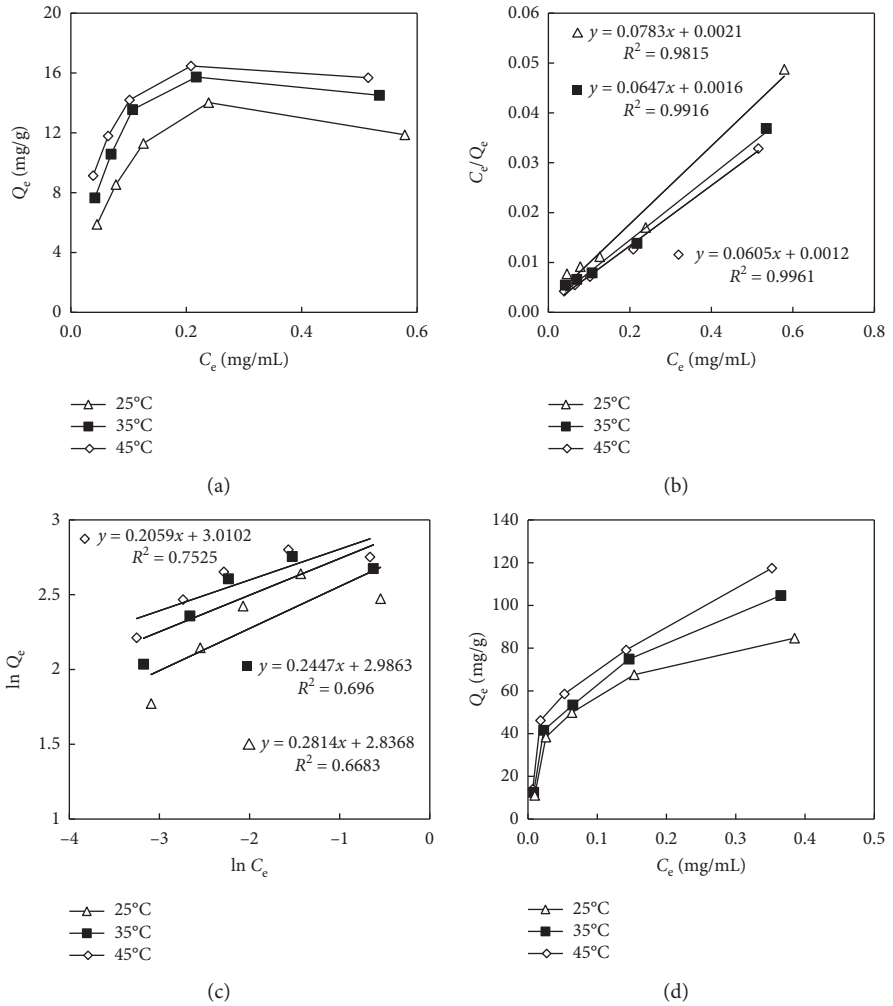

Figure 5: Continued.

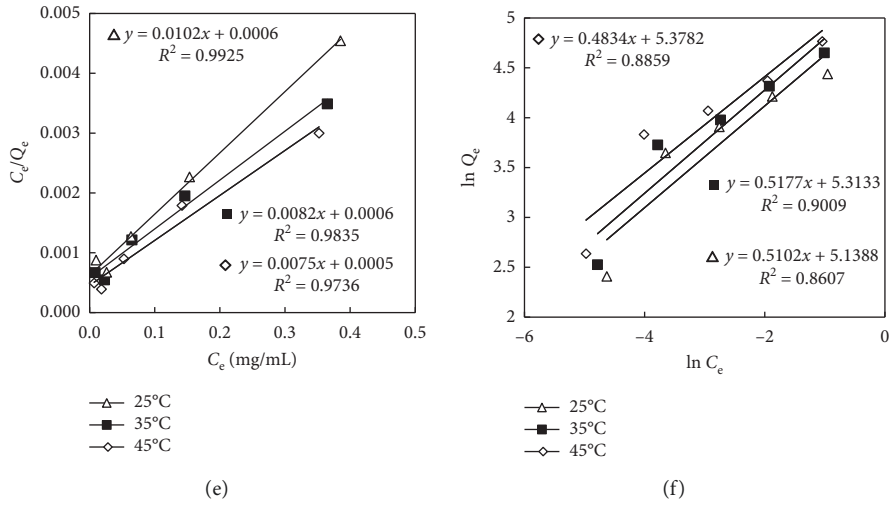

Figure 5: Adsorption isotherms (a, d), fitting result by the Langmuir equation (b, e), and Freundlich equation (c, f) for syringoside and oleuropein, respectively, on the HPD-100B resin at 25, 35, and 45°C.

Table 2: Langmuir and Freundlich adsorption equations of syringoside and oleuropein on the HPD-100B resin at different temperatures.

	Temperature (°C)	Langmuir equation	R^2	Freundlich equation	R^2
Syringoside	25	$C_e/Q_e = 0.0605C_e + 0.0012$	0.9961	$Q_e = 1.102C_e^{0.2059}$	0.7525
	35	$C_e/Q_e = 0.0647C_e + 0.0016$	0.9916	$Q_e = 1.094C_e^{0.2447}$	0.696
	45	$C_e/Q_e = 0.0783C_e + 0.0021$	0.9815	$Q_e = 1.043C_e^{0.2814}$	0.6683
Oleuropein	25	$C_e/Q_e = 0.0075C_e + 0.0005$	0.9736	$Q_e = 1.682C_e^{0.4834}$	0.8859
	35	$C_e/Q_e = 0.0082C_e + 0.0006$	0.9835	$Q_e = 1.670C_e^{0.5177}$	0.9009
	45	$C_e/Q_e = 0.0102C_e + 0.0006$	0.9925	$Q_e = 1.637C_e^{0.5102}$	0.8607

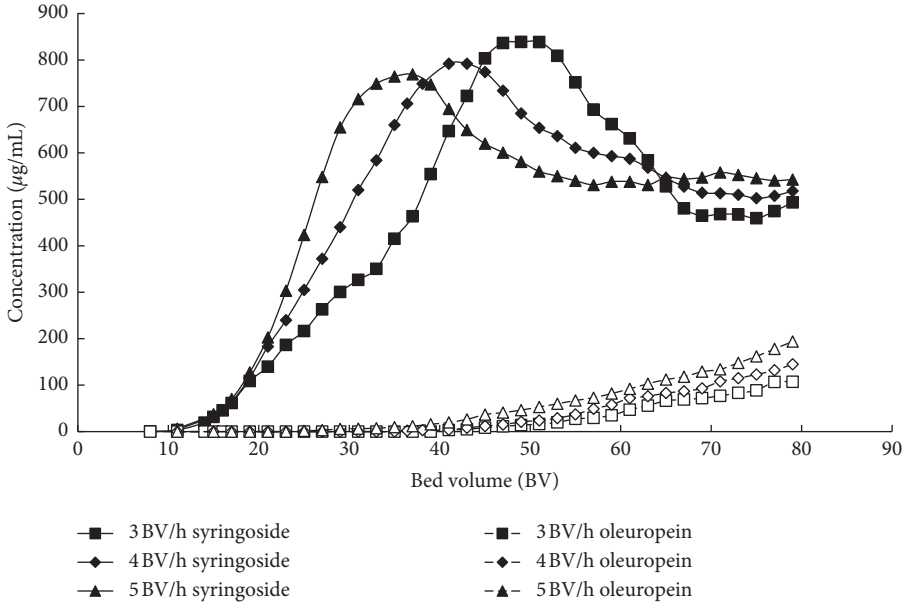

Figure 6: Breakthrough curves of syringoside and oleuropein at different flow rates.

reduce the elution efficiency. Therefore, 3 BV/h is the optimal elution flow rate. The syringoside adsorbed in the resin column can be eluted by collecting 7 BV of the eluent with 20% ethanol-water solution and successively eluting with 40% ethanol-water solution. It took about 9 BV to completely elute the oleuropein in the resin column.

The concentrations of syringoside and oleuropein in the sample solution before and after treatment with the HPD-100B

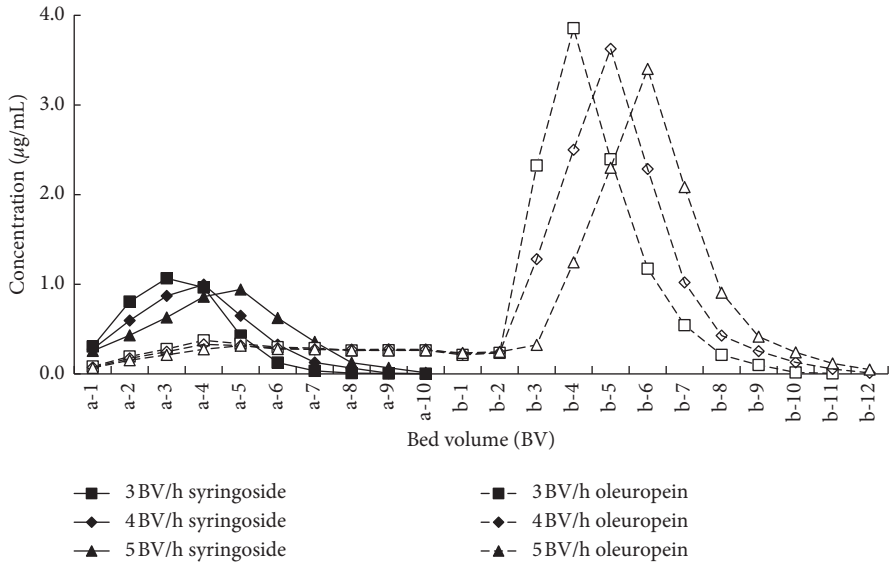

Figure 7: Desorption curves of syringoside and oleuropein with different flow rates; a series in the *X*-axis represent 20% ethanol elution; b series in *X*-axis represent 40% ethanol elution.

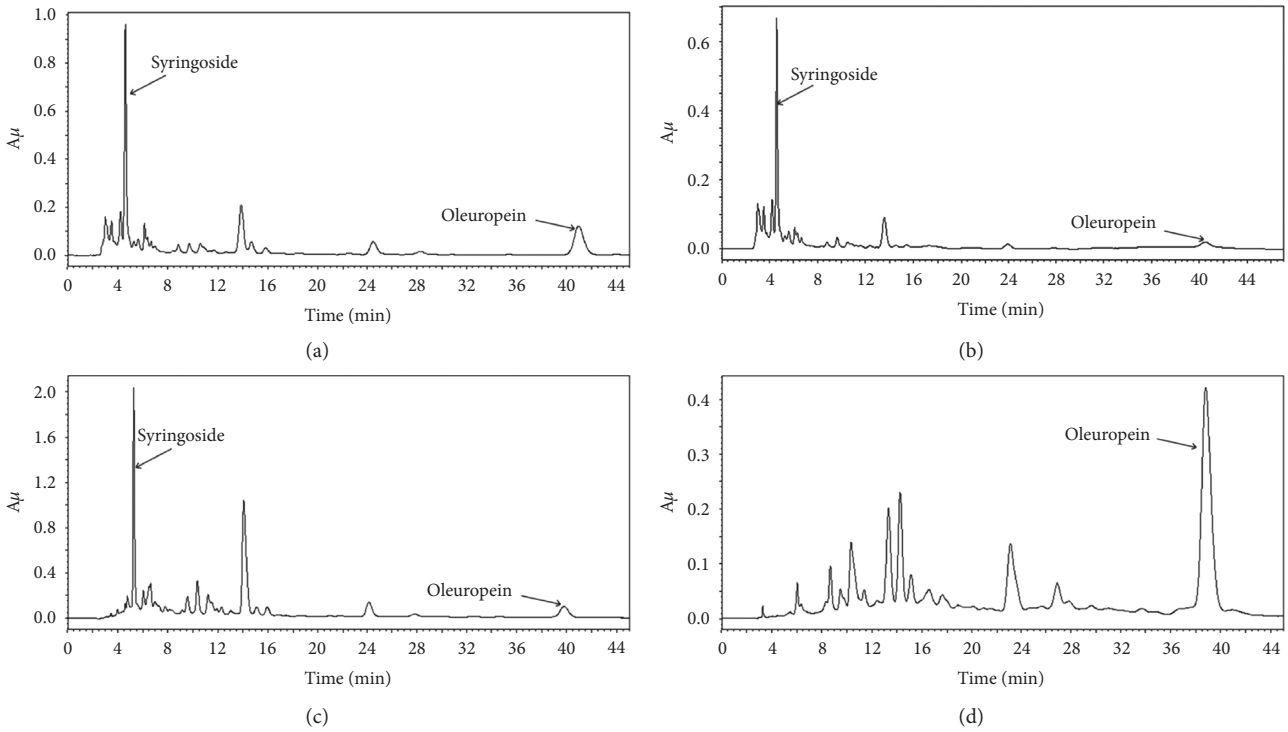

Figure 8: Chromatograms of the sample solution before and after treatment with the HPD-100B resin; (a) before treatment; (b) the effluent from the resin column (15 BV–60 BV); (c) 20% ethanol elution; (d) 40% ethanol elution.

resin were analyzed by HPLC. It can be observed that the relative peak area of syringoside and oleuropein increased significantly after treatment with the HPD-100B resin (Figures 8(a)–8(d)).

In addition, because of the time difference between the adsorption breakthrough points of the two components, effluent with a high syringoside content was obtained by merging 15 BV and 60 BV at 3 BV/h; the quantity of impurities was very low in this solution. The merged liquid can be used for further syringoside purification research. The chromatogram of the merged liquid is shown in Figure 8(b). The concentration of the syringoside in this solution was 0.57 mg/mL, which was equal to 34.4 mg/g of resin. This is much higher than the amount of syringoside adsorbed in the resin column (12.2 mg/g resin). The eluents eluted with 20% ethanol and the effluent (15–60 BV) were merged for the

production of syringoside. After calculation, the syringoside and oleuropein contents in the products increased by 7.2% and 14.2%, respectively, which were 7.1-fold and 8.2-fold higher than those before treatment with the column. The recoveries of syringoside and oleuropein were 77.4% and 89.8%, respectively.

4. Conclusions

By comparing the ability of 11 macroporous resins to adsorb and desorb syringoside and oleuropein from *S. oblata* twig extract, HPD-100B was selected as the ideal resin for the separation and enrichment of the two target components. The static adsorption equilibria of syringoside and oleuropein on the HPD-100B resin were well fitted to the Langmuir isotherm model at various temperatures. Optimal separation conditions were achieved by the following kinetic and dynamic adsorption/desorption experiments: 60 BV loading amount of adsorption at 25°C with a flow rate of 3 BV/h, followed by desorption with a gradient elution of 20% ethanol (7 BV) and 40% ethanol (9 BV) at 25°C and 3 BV/h. It is notable that the adsorption effluent (15 BV–60 BV) contained a high amount of syringoside and low amounts of impurities; therefore, this part was collected for further syringoside separation and purification. The purity of syringoside and oleuropein obtained under the optimized conditions increased by 7.1-fold and 8.2-fold compared with that of the initial extract. The recoveries of syringoside and oleuropein were 77.4% and 89.8%, respectively. This method can be a practical approach for bulk extraction and purification of syringoside and oleuropein in an economical way. As the amazing physiological and pharmacological properties of oleuropein and syringoside, our study provides a means of expanding the alternative sources of syringoside and oleuropein, thereby increasing the additional value of the products.

Data Availability

The data used to support the findings of this study are available from the corresponding author upon request.

Conflicts of Interest

The authors declare that they have no conflicts of interest regarding the publication of this article.

Acknowledgments

This work was funded by the National Key R&D Program of China (2018YFD0600405) and the Program for Young Scholars with Creative Talents in Heilongjiang Bayi Agricultural University (CXRC2017006).

References

[1] H.-S. Niu, I.-M. Liu, J.-T. Cheng, C.-L. Lin, and F.-L. Hsu, "Hypoglycemic effect of syringin from *Eleutherococcus senticosus* in streptozotocin-induced diabetic rats," *Planta Medica*, vol. 74, no. 2, pp. 109–113, 2008.

[2] B. A. Ahmad, K. S. Mohd, M. Abdurazak, U. Rao, and T. Zin, "Phytochemical screening, antioxidant activity of pure syringin in comparison to various solvents extracts of *Musa paradisiaca* (banana) (fruit and flower) and total phenolic contents," *International Journal of Pharmacy and Pharmaceutical Sciences*, vol. 7, no. 5, pp. 242–247, 2015.

[3] J. Y. Cho, K. H. Nam, A. R. Kim et al., "In-vitro and in-vivo immunomodulatory effects of syringin," *Journal of Pharmacy and Pharmacology*, vol. 53, no. 9, pp. 1287–1294, 2001.

[4] J. Choi, K.-M. Shin, H.-J. Park et al., "Anti-inflammatory and antinociceptive effects of sinapyl alcohol and its glucoside syringin," *Planta Medica*, vol. 70, no. 11, pp. 1027–1032, 2004.

[5] M. Ahmad and K. Aftab, "Hypotensive action of syringin from *Syringa vulgaris*," *Phytotherapy Research*, vol. 9, no. 6, pp. 452–454, 1995.

[6] Y. Cui, Y. Zhang, and G. Liu, "Syringin may exert sleep-potentiating effects through the NOS/NO pathway," *Fundamental & Clinical Pharmacology*, vol. 29, no. 2, pp. 178–184, 2015.

[7] X. Gong, L. Zhang, R. Jiang, C.-D. Wang, X.-R. Yin, and J.-Y. Wan, "Hepatoprotective effects of syringin on fulminant hepatic failure induced by D-galactosamine and lipopolysaccharide in mice," *Journal of Applied Toxicology*, vol. 34, no. 3, pp. 265–271, 2014.

[8] E. Longo, K. Morozova, and M. Scampicchio, "Effect of light irradiation on the antioxidant stability of oleuropein," *Food Chemistry*, vol. 237, no. 15, pp. 91–97, 2017.

[9] P. M. Furneri, A. Marino, A. Saija, N. Uccella, and G. Bisignano, "In vitro antimycoplasmal activity of oleuropein," *International Journal of Antimicrobial Agents*, vol. 20, no. 4, pp. 293–296, 2002.

[10] E. Haloui, B. Marzouk, Z. Marzouk, A. Bouraoui, and N. Fenina, "Hydroxytyrosol and oleuropein from olive leaves: potent anti-inflammatory and analgesic activities," *Journal of Food, Agriculture & Environment*, vol. 9, no. 3-4, pp. 128–133, 2011.

[11] A. Ahmad Farooqi, S. Fayyaz, A. Silva et al., "Oleuropein and cancer chemoprevention: the link is hot," *Molecules*, vol. 22, no. 5, p. 705, 2017.

[12] M. Imran, M. Nadeem, S. A. Gilani, S. Khan, M. W. Sajid, and R. M. Amir, "Antitumor perspectives of oleuropein and its metabolite hydroxytyrosol: recent updates," *Journal of Food Science*, vol. 83, no. 7, pp. 1781–1791, 2018.

[13] S. H. Omar, "Cardioprotective and neuroprotective roles of oleuropein in olive," *Saudi Pharmaceutical Journal*, vol. 18, no. 3, pp. 111–121, 2010.

[14] M. Sumiyoshi and Y. Kimura, "Effects of olive leaf extract and its main component oleuroepin on acute ultraviolet B irradiation-induced skin changes in C57BL/6J mice," *Phytotherapy Research*, vol. 24, no. 7, pp. 995–1003, 2010.

[15] Y. Kimura and M. Sumiyoshi, "Olive leaf extract and its main component oleuropein prevent chronic ultraviolet B radiation-induced skin damage and carcinogenesis in hairless mice," *The Journal of Nutrition*, vol. 139, no. 11, pp. 2079–2086, 2009.

[16] X. Liu, X. Jing, and G. Li, "Optimization of vacuum microwave-mediated extraction of syringoside and oleuropein from twigs of *Syringa oblata*," *Journal of Analytical Methods in Chemistry*, vol. 2018, Article ID 6179013, 9 pages, 2018.

[17] M. Chen, M. Zou, A. Li, Z. Qu, F. Wang, and F. Tian, "Study on purity and characterization of syringin standard material," *Food Science*, vol. 23, no. 7, pp. 121–123, 2002.

[18] J. Yan, S. Tong, J. Chu, L. Sheng, and G. Chen, "Preparative isolation and purification of syringin and edgeworoside C from *Edgeworthia chrysantha* Lindl by high-speed counter-

current chromatography," *Journal of Chromatography A*, vol. 1043, no. 2, pp. 329–332, 2004.

[19] Z.-Q. Wu, G.-Z. Yue, Q.-P. Zhu et al., "Purification, dynamic changes and antioxidant activities of oleuropein in olive (*Olea europaea* L.) leaves," *Journal of Food Biochemistry*, vol. 39, no. 5, pp. 566–574, 2015.

[20] Y. Bai, J. Ma, W. Zhu et al., "Highly selective separation and purification of chicoric acid from *Echinacea purpurea* by quality control methods in macroporous adsorption resin column chromatography," *Journal of Separation Science*, vol. 42, no. 5, pp. 1027–1036, 2019.

[21] N. Xiong, R. Yu, T. Chen, Y.-P. Xue, Z.-Q. Liu, and Y.-G. Zheng, "Separation and purification of l-methionine from *E. coli* fermentation broth by macroporous resin chromatography," *Journal of Chromatography B*, vol. 1110-1111, pp. 108–115, 2019.

[22] M. L. Soto, A. Moure, H. Domínguez, and J. C. Parajó, "Recovery, concentration and purification of phenolic compounds by adsorption: a review," *Journal of Food Engineering*, vol. 105, no. 1, pp. 1–27, 2011.

[23] M. Anvari and G. Khayati, "Separation and purification of rebaudioside A from extract of *Stevia rebaudiana* leaves by macroporous adsorption resins," *Polish Journal of Chemical Technology*, vol. 18, no. 1, pp. 127–132, 2016.

[24] Y. Dong, M. Zhao, D. Sun-Waterhouse et al., "Absorption and desorption behaviour of the flavonoids from *Glycyrrhiza glabra* L. leaf on macroporous adsorption resins," *Food Chemistry*, vol. 168, pp. 538–545, 2015.

[25] T. T. Bien, B. T. T. Luyen, and N. V. Han, "Preparative separation and purification of geniposide from *Gardenia jasminoides* ellis fruit using macroporous adsorption resin D101," *Pharmaceutical Sciences Asia*, vol. 42, no. 1, pp. 29–36, 2018.

[26] C. Gao, S. Zhao, Y. Yagiz, and L. Gu, "Static, kinetic, and isotherm adsorption performances of macroporous adsorbent resins for recovery and enrichment of bioactive procyanidins from cranberry pomace," *Journal of Food Science*, vol. 83, no. 5, pp. 1249–1257, 2018.

[27] C. Wang, Z. Chao, X. Wu, W. Sun, and Y. Ito, "Enrichment and purification of pedunculoside and syringin from the barks of *Ilex rotunda* with macroporous resins," *Journal of Liquid Chromatography & Related Technologies*, vol. 37, no. 4, pp. 572–587, 2013.

[28] L. Yao, L. Wang, B. Zhao et al., "Separation of syringin and flavonoids from *Saussurea involucrata* by macroporous resin," *Asian Journal of Chemistry*, vol. 24, no. 2, pp. 871–876, 2012.

[29] S. Şahin and M. Bilgin, "Selective adsoprtion of oleuropein from olive (*Olea europaea*) leaf extract by using macroporous resin," *Chemical Engineering Communications*, vol. 204, no. 12, pp. 1391–1400, 2017.

[30] N. Xynos, G. Papaefstathiou, M. Psychis, A. Argyropoulou, N. Aligiannis, and A.-L. Skaltsounis, "Development of a green extraction procedure with super/subcritical fluids to produce extracts enriched in oleuropein from olive leaves," *The Journal of Supercritical Fluids*, vol. 67, pp. 89–93, 2012.

[31] F. Yang, L. Yang, W. Wang, Y. Liu, C. Zhao, and Y. Zu, "Enrichment and purification of syringin, eleutheroside E and isofraxidin from *Acanthopanax senticosus* by macroporous resin," *International Journal of Molecular Sciences*, vol. 13, no. 7, pp. 8970–8986, 2012.

[32] B. Liu, B. Dong, X. Yuan et al., "Enrichment and separation of chlorogenic acid from the extract of *Eupatorium adenophorum* Spreng by macroporous resin," *Journal of Chromatography B*, vol. 1008, pp. 58–64, 2016.

[33] M. Bilal, S.-J. Yue, H.-B. Hu, W. Wang, and X.-H. Zhang, "Adsorption/desorption characteristics, separation and purification of phenazine-1-carboxylic acid from fermentation extract by macroporous adsorbing resins," *Journal of Chemical Technology & Biotechnology*, vol. 93, no. 11, pp. 3176–3184, 2018.

[34] M. Gao, W. Huang, and C.-Z. Liu, "Separation of scutellarin from crude extracts of *Erigeron breviscapus* (vant.) Hand. Mazz. by macroporous resins," *Journal of Chromatography B*, vol. 858, no. 1-2, pp. 22–26, 2007.

[35] T. W. Charpe and V. K. Rathod, "Separation of glycyrrhizic acid from licorice root extract using macroporous resin," *Food and Bioproducts Processing*, vol. 93, pp. 51–57, 2015.